A Thin-Layer Model for Viscoelastic, Stress-Relaxation Testing of Cells Using Atomic Force Microscopy: Do Cell Properties Reflect Metastatic Potential?

Eric M. Darling,*†§ Stefan Zauscher,‡§ Joel A. Block,¶ and Farshid Guilak*†‡§

Departments of *Surgery, †Biomedical Engineering, and ‡Mechanical Engineering and Materials Science, and §Center for Biomolecular and Tissue Engineering, Duke University Medical Center, Durham, North Carolina; and ¶Department of Internal Medicine, Rush University Medical Center, Chicago, Illinois

ABSTRACT Atomic force microscopy has rapidly become a valuable tool for quantifying the biophysical properties of single cells. The interpretation of atomic force microscopy-based indentation tests, however, is highly dependent on the use of an appropriate theoretical model of the testing configuration. In this study, a novel, thin-layer viscoelastic model for stress relaxation was developed to quantify the mechanical properties of chondrosarcoma cells in different configurations to examine the hypothesis that viscoelastic properties reflect the metastatic potential and invasiveness of the cell using three well-characterized human chondrosarcoma cell lines (JJ012, FS090, 105KC) that show increasing chondrocytic differentiation and decreasing malignancy, respectively. Single-cell stress relaxation tests were conducted at 2 h and 2 days after plating to determine cell mechanical properties in either spherical or spread morphologies and analyzed using the new theoretical model. At both time points, JJ012 cells had the lowest moduli of the cell lines examined, whereas FS090 typically had the highest. At 2 days, all cells showed an increase in stiffness and a decrease in apparent viscosity compared to the 2-h time point. Fluorescent labeling showed that the F-actin structure in spread cells was significantly different between FS090 cells and JJ012/105KC cells. Taken together with results of previous studies, these findings indicate that cell transformation and tumorigenicity are associated with a decrease in cell modulus and apparent viscosity, suggesting that cell mechanical properties may provide insight into the metastatic potential and invasiveness of a cell.

INTRODUCTION

Viscoelastic mechanical properties of single cells have been quantified using a variety of testing methods, including micropipette aspiration, cytoindentation, magnetic bead rheometry, optical traps, and AFM (1–7). In particular, AFM provides an advantage over some of these techniques in that the mechanical properties of adherent cells can be tested in different geometries following cell adhesion (i.e., from spherical to flattened shapes). The interpretation of AFM-based indentation tests on single cells, however, is highly dependent on the use of an appropriate theoretical model of the contact geometry. For example, one potential limitation of this approach is that indentation testing of highly flattened cells may violate the assumption of infinitesimal strain in a thin layer. Experimentally, however, an advantage of AFM is the ability to precisely control cantilever movement, and thus, indirectly, indentation depth, which, in combination with an appropriate theoretical model, can be used to test very thin layers without violating the small-strain assumptions typically made in indentation models (3,8,9).

The viscoelastic properties and deformation behavior of cells play important roles in many biophysical and biological responses (see reviews in (10–14)). For example, metastasis of cancerous cells involves a complex sequence of interlinked biochemical and biomechanical events, including cell adhesion, migration, and deformation during tumor cell invasion (7,15), suggesting that the metastatic potential of a cell may be directly dependent on its mechanical properties. In patients with chondrosarcoma, metastatic spread is the primary cause of death, and human chondrosarcomas are known to vary widely in their biological behavior and histological appearance, making it difficult to identify the likelihood of metastasis in a patient (16). These populations of cartilage-forming cells typically arise in benign cartilage neoplasms, enchondromas, or osteochondromas (17). At times, these growths can rapidly enlarge and metastasize, subsequently destroying healthy tissue throughout the body. However, difficulties arise in diagnosing the malignancy of this cancer, because no clear histopathology exists for identifying the metastatic potential of chondrosarcoma cells.

Submitted February 9, 2006, and accepted for publication November 27, 2006.

Address reprint requests to Farshid Guilak, Orthopaedic Research Laboratories, 375 MSRB, Box 3093, Duke University Medical Center, Durham, NC 27710. Tel.: 919-684-2521; Fax: 919-681-8490; E-mail: guilak@duke.edu.

Abbreviations used: AFM, atomic force microscopy; $E_{elastic}$, elastic modulus (from Hertz model); E_{equil}, equilibrium modulus (from Hertz model at 60 s); F, force; h, height of cell; δ, indentation; E_0, instantaneous modulus; k_1, k_2, Kelvin spring elements; μ, Kelvin viscous element, apparent viscosity; G, modulus of rigidity; ν, Poisson's ratio; R_{probe}, radius of probe tip; R, relative radius; E_R, relaxed modulus; ε, strain; σ, stress; τ_σ, time of relaxation of deformation under constant load; τ_ε, time of relaxation of load under constant deformation; α, thin-layer model constants; function of the Poisson's ratio; χ, thin-layer model variable, $\chi = \sqrt{R\delta}/h$; E_Y, Young's modulus.

0006-3495/07/03/1784/08 $2.00

doi: 10.1529/biophysj.106.083097

Previous studies have investigated how cells from different types of chondrosarcomas vary based on biosynthesis or gene expression (17–24). The aggressiveness of a cell line was shown to be related inversely to its degree of differentiation with respect to the normal chondrocyte phenotype. For example, more malignant and invasive cell lines exhibited no keratan sulfate substitution into glycosaminoglycan chains and possessed a high expression of type-I collagen with almost no expression of type-II collagen (24). Furthermore, the metastatic ability of chondrosarcoma cells was found to be related to their collagenase (MMP-1) activity, which helps degrade cartilaginous tissue in the primary tumor as well as in the vasculature at the site of metastatic invasion. Relevant studies have shown that more aggressive cancers have the ability to deform and squeeze through tissue matrix to access the circulatory system and subsequently move through small leaks in blood vessel walls to establish new tumors (25,26). These findings suggest that the metastatic potential of a cancer cell may be related to the biomechanical properties that influence the process of cell escape from the compartment of origin and subsequent penetration into other remote tissues. Although the biological characteristics of chondrosarcoma cells have been investigated, their mechanical properties are as yet unknown.

The goal of this study was to develop a new thin-layer, AFM stress relaxation model to determine the viscoelastic mechanical properties of chondrosarcoma cells in both their rounded and spread morphologies. The mechanical properties of cells from different lines were hypothesized to correlate with their documented invasiveness and metastatic potential. Specifically, it was hypothesized that more invasive cell lines exhibit higher deformability (i.e., lower modulus), reflecting intrinsic differences in cytoskeletal structure. Three well-characterized human chondrosarcoma cell lines of varying aggressiveness were mechanically tested using AFM. The viscoelastic properties of both rounded and flattened chondrosarcoma cells were determined by fitting a model of stress relaxation indentation of a thin layer to the experimental data.

MATERIALS AND METHODS

Chondrosarcoma culture conditions

Three human chondrosarcoma cell lines that previously have been characterized biochemically and found to have stable phenotypes with differing levels of invasiveness and metastatic potential were investigated in this study: JJ012, FS090, and 105KC (17–24). Cell lines were cultured in monolayer at 37°C and 5% CO_2 for >2 weeks before being tested. Culture media consisted of high glucose Dulbecco's modified eagle medium (Gibco, Carlsbad, CA), 1× penicillin/streptomycin (Gibco), and 10% fetal bovine serum (Gibco). Initially, chondrosarcoma cells from each line were released from tissue-culture treated flasks using 0.05% trypsin (Gibco), washed thoroughly in culture media, and seeded either onto a poly-L-lysine (PLL) coated slide or 35-mm petri dish. Cells on PLL slides were tested with the AFM ~2 h after seeding, whereas cells in 35-mm petri dishes were tested 2 days after seeding. Short seeding times provided a consistent testing morphology (spherical) that allowed all cell lines to be compared without having to account for major differences in cell shape. Long seeding times allowed the chondrosarcoma cells to equilibrate metabolically and attain a more ''native'' state. Three separate testing sessions were performed for each time point.

Atomic force microscopy

The biomechanical properties of chondrosarcoma cells were measured using an atomic force microscope (MFP-3D, Asylum Research, Santa Barbara, CA) that allows closed-loop feedback position control in the z-direction. This programmability enabled the AFM to maintain nearly constant indentation displacement while conducting a stress relaxation test. To determine the indentation force applied to a cell, the deflection of the cantilever tip was monitored by tracking the position of a laser beam reflected off the cantilever tip onto a photosensitive detector. The applied force was determined by multiplying the cantilever stiffness by its deflection via Hooke's law ($F = kx$).

Cantilevers modified with a borosilicate glass sphere (5 μm nominal diameter, Novascan Technologies, Ames, IA) were used for the AFM stress relaxation experiments (Fig. 1) (27). Cantilever spring constants (typically 0.065 N/m) were determined from the power spectral density of the thermal noise fluctuations (28) before experimentation. Stress relaxation tests were performed on the central region of a cell using a 6.25-μm/s approach velocity and 60-s relaxation time. For flattened cells, the probe tip was positioned over the cell nuclei to help standardize testing between different cell shapes. Cell heights were determined directly from AFM measurements using cell and substrate contact points. A 2.5-nN trigger force was used to prescribe the point at which the cantilever approach was stopped and held at a constant displacement for the stress relaxation portion of the testing. For most cells, this distance was equivalent to a 1.0 ± 0.3 μm (2 h) or 0.85 ± 0.22 μm (2 days) indentation, which resulted in nominal strains of ~7–13% for cell heights of 14.3 ± 2.1 μm (2 h) or 6.4 ± 1.7 μm (2 days).

The experimental data were analyzed with elastic and viscoelastic models. The indentation approach curves were fit with a thin-layer Hertz equation (Eq. 1) to determine the elastic modulus, $E_{elastic}$. Because of the high rate of indentation, this measurement was assumed to be a better indicator of the instantaneous response of a cell than the viscoelastic parameter E_0. The equilibrium modulus, E_{equil}, was also calculated using the Hertz equation but with the force measurement after 60 s. Data from the relaxation phase of the test were fit with the thin-layer, viscoelastic equation (Eq. 3) to determine E_R, τ_σ, and τ_ε. E_0, μ, E_Y, k_1, and k_2 were calculated

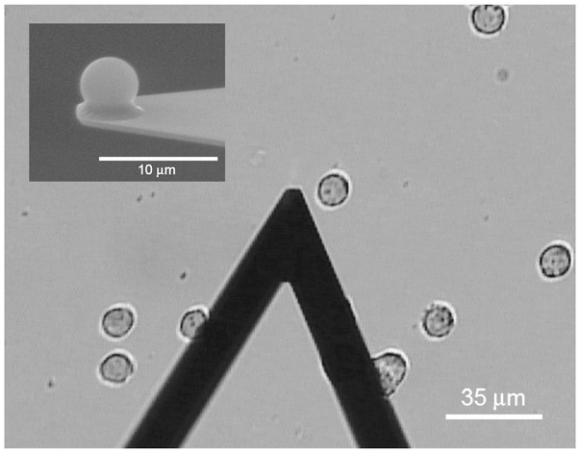

FIGURE 1 Single-cell indentation using AFM. Individual chondrosarcoma cells were indented with a 5-μm diameter sphere. Stress relaxation experiments were conducted for each of three cell lines: JJ012, FS090, and 105KC. Pictured above are JJ012 cells at 2 h after seeding onto PLL-coated, glass slides.

using Eqs. 4–5, which are described in the following section. Linear drift in the laser was accounted for during data analysis using an algebraic correction. The Poisson's ratio, ν, was assumed to be 0.38, based on previous studies of chondrocytes (5,29,30).

Thin-layer, stress relaxation model for AFM

A common method for determining the viscoelastic characteristics of a material is to measure the stress relaxation response to a prescribed displacement. In this AFM-based study, we indented a cell with an approximate step displacement and recorded the resulting force response over time. Because force is determined via cantilever deflection, a small indentation change (<1% of total indentation) does occur during the initial drop in stress. Instead of a constant strain, the actual input mimics an inverted relaxation response on a much smaller scale (inverted Fig. 2). The magnitude of this change is such that a constant strain condition can be assumed. The force-displacement data were then fit with an indentation model, which assumes an infinitely hard sphere indenting a flat, deformable substrate, and can be described by a thin-layer, Hertz model (31):

$$F = \frac{4E_Y R^{1/2}}{3(1-\nu^2)}\delta^{3/2}\left[1 - \frac{2\alpha_0}{\pi}\chi + \frac{4\alpha_0^2}{\pi^2}\chi^2 - \frac{8}{\pi^3}\left(\alpha_0^3 + \frac{4\pi^2}{15}\beta_0\right)\chi^3 + \frac{16\alpha_0}{\pi^4}\left(\alpha_0^3 + \frac{3\pi^2}{5}\beta_0\right)\chi^4\right],$$
$$R = \left(\frac{1}{R_{\text{probe}}} + \frac{1}{h/2}\right)^{-1}, \quad (1)$$

where F is the applied force, E_Y is the Young's modulus, R is the relative radius (for flat surfaces such as spread cells $R = R_{\text{probe}}$) (32), R_{probe} is the probe radius, h is cell height, ν is Poisson's ratio, δ is the indentation, $\chi = \sqrt{R\delta}/h$, and the constants α_0 and β_0 are functions of the Poisson's ratio, which for a material bonded to a surface are defined as:

$$\alpha_0 = -\frac{1.2876 - 1.4678\nu + 1.3442\nu^2}{1-\nu},$$
$$\beta_0 = \frac{0.6387 - 1.0277\nu + 1.5164\nu^2}{1-\nu}. \quad (2)$$

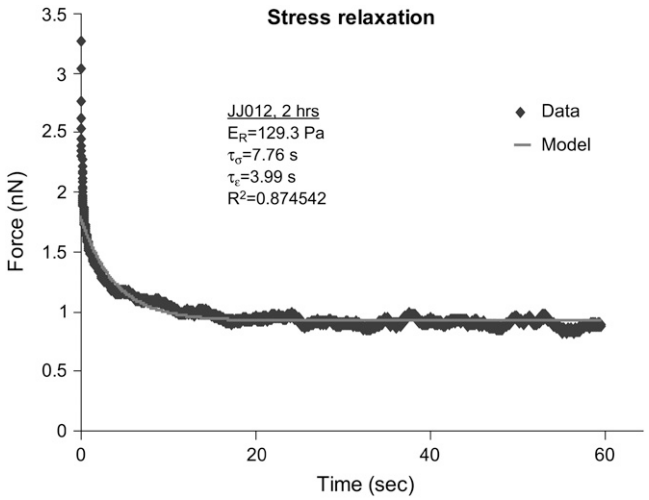

FIGURE 2 Stress relaxation response with thin-layer, viscoelastic model. The thin-layer mathematical model closely described the viscoelastic response of single cells to a constant strain condition. Stress relaxation tests were conducted for 60 s, after which fit parameters were extracted from the data to help characterize the mechanical properties of the chondrosarcoma cell lines.

The thin-layer Hertz equation (Eq. 1), when used with the initial indentation phase of the data, describes the elastic response of a soft material (31).

For the stress relaxation tests, an approximately constant strain is applied to the cells while the force is recorded over time (Fig. 2). The bracketed expression in Eq. 1 is essentially one large constant because it depends only on the indentation and is therefore assumed to be constant during stress relaxation. To obtain a thin-layer, viscoelastic model appropriate for stress relaxation, we can append this ''thin-layer correction'' to the AFM indentation solution derived by Darling et al. (27). The final model is applicable to small indentations of an isotropic, incompressible surface with a hard, spherical indenter:

$$F(t) = \frac{4R^{1/2}\delta_0^{3/2}E_R}{3(1-\nu)}\left(1 + \frac{\tau_\sigma - \tau_\varepsilon}{\tau_\varepsilon}e^{-t/\tau_\varepsilon}\right)C,$$
$$C = \left[1 - \frac{2\alpha_0}{\pi}\chi + \frac{4\alpha_0^2}{\pi^2}\chi^2 - \frac{8}{\pi^3}\left(\alpha_0^3 + \frac{4\pi^2}{15}\beta_0\right)\chi^3 + \frac{16\alpha_0}{\pi^4}\left(\alpha_0^3 + \frac{3\pi^2}{5}\beta_0\right)\chi^4\right], \quad (3)$$

where $\chi = \sqrt{R\delta_0}/h$ and τ_σ and τ_ε are the relaxation times under constant load and deformation, respectively. Fitting Eq. 3 to a force-displacement curve provides three parameters that describe a cell's viscoelastic response as a standard linear solid (a spring-dashpot in parallel with another spring):

$$k_1 = E_R,$$
$$k_2 = E_R\frac{(\tau_\sigma - \tau_\varepsilon)}{\tau_\varepsilon}, \quad \text{and}$$
$$\mu = E_R(\tau_\sigma - \tau_\varepsilon), \quad (4)$$

where k_1 and k_2 are Kelvin spring elements and μ is a damper element and describes the apparent viscosity. The instantaneous and Young's moduli can then be calculated:

$$E_0 = E_R\left(1 + \frac{\tau_\sigma - \tau_\varepsilon}{\tau_\varepsilon}\right) \quad \text{and}$$
$$E_Y = \frac{3}{2}E_R. \quad (5)$$

The thin-layer model is appropriate for samples where $h \leq 12.8R$ (31), which in this study includes both rounded (2 h) and flattened (2 days) cells because neither are taller than 23 μm. The curvature associated with spherical cells are accounted for using a relative radius, whereas spread cells are assumed to have a flat surface. The geometry of the sample does not otherwise affect the data analysis as long as applied strains are $<\sim$10%. AFM data from all samples were fit to Eqs.1 and 3 to determine the elastic and viscoelastic properties of single, chondrosarcoma cells.

Apparent membrane area

The apparent membrane area of cells from each cell line was determined using an osmotic swelling method, as described previously (33). Approximately 1 ml of cell suspension was placed into a specially designed chamber that allowed for the entry of the micropipette from the side (1). The chamber was mounted on a translating stage that allowed the entire chamber and solution to be rapidly replaced while a micropipette held a single cell stationary in the viewing field of the microscope. Chondrosarcoma cells were held stationary with a glass micropipette in a chamber containing isoosmotic solution. The micropipette was then inserted inside a large

micropipette (~50 μm diameter) to minimize perturbations to the cell during transfer to a new chamber (2). The chamber was rapidly replaced by an adjacent chamber containing deionized water, and the larger micropipette was then removed. Cell swelling was recorded at video rates (60 fields/s) until lysis using a video camera (model XC-77, Hamamatsu Photonic System, Bridgewater, NJ) through a bright-field microscope (Leitz Diavert, Rockleigh, NJ), using a 100× oil immersion objective of 1.25 N.A. (Carl Zeiss, Thornwood, NY). Cell diameter was measured as the mean of the horizontal and vertical diameters and was measured from videotape using a video dimensional analysis system (Vista Electronics, Ramona, CA). Cell volume and surface area were calculated from the cell diameter assuming a spherical geometry. The apparent ''excess'' membrane area was calculated as the maximum change in the cell surface area between the isoosmotic solution and deionized water.

Cytoskeletal F-actin imaging

The organization of the F-actin cytoskeleton of chondrosarcoma cells was investigated using Alexa Fluor 488 phalloidin (Molecular Probes, Eugene, OR), a fluorescent phallotoxin that stains for F-actin. Briefly, cells from each line were seeded onto glass, four-chamber, coverslip slides (Nunc, Rochester, NY) and allowed to attach for either 2 h or 2 days. The attached cells were then gently washed with PBS (Gibco) before being fixed with 3.4% formaldehyde (Ricca Chemical, Arlington, TX) for 10 min. The samples were again washed with PBS and then permeabilized by exposure to acetone for 5 min at −20°C. After another wash, the samples were blocked with 1% BSA (Gibco) for 30 min then exposed to a 0.33 μM solution of Alexa Fluor 488 phalloidin in 1% BSA for 20 min. Samples were washed once more before being imaged on a confocal microscope with excitation of 495 nm and emission recorded at 519 nm using a 63× (1.3 NA) water immersion objective lens (LSM 510, Zeiss, Thornwood, NY).

Statistical analysis

A sample size of $n > 26$ cells was used for each experimental group and time point. Two-factor ANOVA was conducted to determine whether significant differences existed, with statistical significance reported at the 95% confidence level ($p < 0.05$), among the biomechanical properties of the cell lines (FS090, 105KC, JJ012) at two different culture times (2 h and 2 days). If significance existed, a post-hoc analysis was performed using the Newman-Keuls test to determine significance for multiple comparisons.

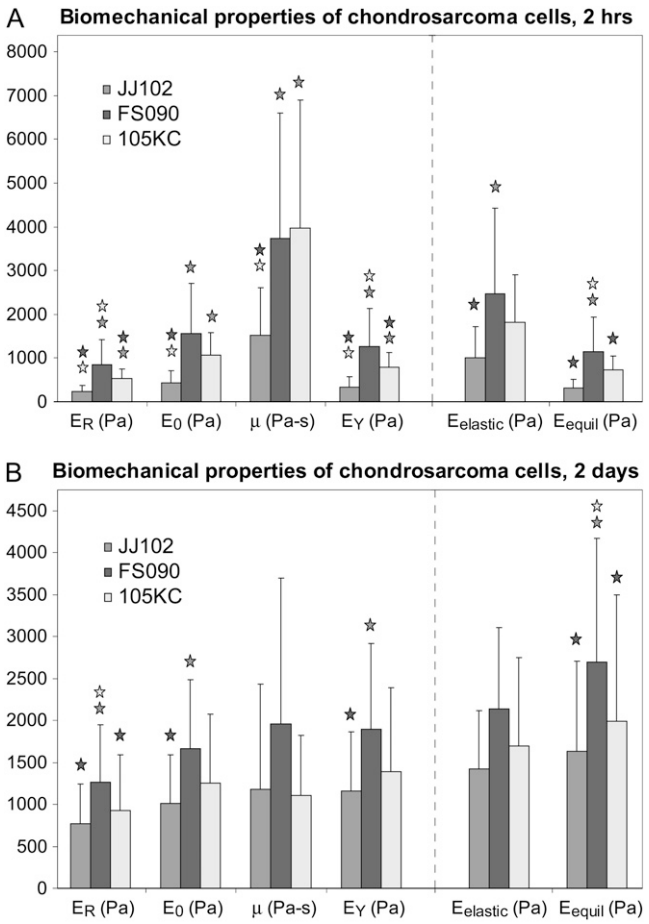

FIGURE 3 Biomechanical properties of JJ012, FS090, and 105KC chondrosarcoma cell lines. Moduli and apparent viscosities (mean ± SD) were determined for each cell by fitting the stress relaxation data with the thin-layer elastic and viscoelastic models. The relaxed, instantaneous, and elastic moduli at 2 h all followed the same progression with JJ012<105KC<FS090 (*A*). At 2 days, a similar trend was observed, although JJ012 and 105KC cell properties were more similar to each other (*B*). Significance between cell lines ($p < 0.05$) is indicated by a corresponding colored star above the mechanical property (e.g., E_{equil} at 2 h is significant between FS and JJ or KC, but E_{equil} at 2 h is not significant between JJ and KC).

RESULTS

Biomechanical properties

Biomechanical properties varied significantly among cells from all lines at 2 h after seeding (Fig. 3 *A*). FS090 cells were the stiffest, with a Young's modulus of 1.27 ± 0.86 kPa. The modulus of 105KC and JJ012 cells were only 62% and 27% that of FS090 cells ($p < 0.05$). This ranking of mechanical properties was consistent for all measured values except apparent viscosity. For this property, both FS090 and 105KC cells proved to be significantly ($p < 0.0002$) higher than JJ012 cells, but did not vary between themselves ($p = 0.66$). The apparent viscosity of JJ012 cells was ~60% that of the other cell lines.

The material properties of cells seeded for 2 days also showed significant differences between the lines (Fig. 3 *B*). Similar to the 2-h findings, the Young's modulus of JJ012 cells was 63% that of FS090 cells ($p < 0.004$). Between these two cell lines, significant differences were observed for all mechanical properties except the apparent viscosity and elastic modulus, which showed no significant differences among any of the three cell lines. In contrast to the mechanical properties seen at 2 h, 105KC and JJ012 cells displayed similar moduli and apparent viscosities ($p > 0.2$).

In general, moduli recorded from cells cultured for 2 days were higher than those seeded for 2 h, whereas the apparent viscosities were lower for cells tested at the later time point (Fig. 3). The values for E_R, E_0, E_{equil}, and μ showed highly significant increases ($p < 0.0001$) from 2 h to 2 days. The values for E_R, E_0, and E_{equil} all increased as the cells spread in monolayer culture. The apparent viscosities of the cells decreased during this period for FS090 and 105KC cells but not for JJ012 cells. In contrast to these temporal effects, the

elastic modulus, $E_{elastic}$, showed no significant increase or decrease over time ($p = 0.84$). The mathematical models fit the data well for both elastic ($R^2 = 0.99 \pm 0.02$) and viscoelastic ($R^2 = 0.85 \pm 0.13$) tests, although the latter did not accurately represent the earliest stage of stress relaxation, and hence, E_0 values were lower than expected. Mechanical property data not illustrated in Fig. 3 are given in Table 1.

Apparent membrane area

All cells lines showed large amounts of apparent excess membrane area relative to the isoosmotic state. FS090 cells showed significantly greater excess membrane area (3.33 ± 0.53) as compared to 105KC cells (2.70 ± 0.52, $p < 0.0005$) or JJ012 cells (2.48 ± 0.44, $p < 0.0001$). No significant differences were detected between 105KC and JJ012 cells.

Cell morphology and cytoskeletal imaging

The cellular morphology and actin structure for cells seeded for 2 h were similar among all cell lines (Fig. 4, *A–C*). The cells exhibited a spherical shape with F-actin localized to a cortical shell, in addition to a very thin cytoskeletal layer located at the base of the cell (Fig. 5 *A*). Based on AFM measurements, JJ012 and FS090 cell heights (i.e., diameters) were similar (13.1 ± 0.6 μm and 13.1 ± 0.7 μm, respectively) whereas 105KC cells were generally larger (16.6 ± 1.8 μm).

Cellular morphologies at 2 days varied based on cell line, with FS090 cells typically being elongated whereas JJ012 and 105KC cells exhibited less uniform structures (Fig. 4, *D–F*). In general, cells flattened to ~50% of their initial height, spreading in a manner dependent upon cell line (Fig. 5 *B*). Actin fibers were aligned longitudinally in FS090 cells, whereas there was no consistent orientation in JJ012 and 105KC cells. However, 105KC and JJ012 cells typically exhibited tall, central bulges where the nuclei were located, whereas FS090 cells showed more uniform heights with a gradual decrease from center to edge. Due to these morphologies, the measured height at the nucleus was approximately the same for all spread cells (6.4 ± 1.7 μm).

DISCUSSION

The findings of this study show that the viscoelastic properties of chondrosarcoma cells are well characterized by the derived thin-layer, viscoelastic model for stress relaxation indentation. Furthermore, the results indicate that chondrosarcoma mechanical properties may differ significantly among cell lines that exhibit different levels of aggressiveness and metastatic potential, with the most aggressive and invasive cell line, JJ012, showing the lowest modulus. These results provide support for the hypothesis that cell deformability may reflect certain phenotypic characteristics that are related to the metastatic process, such as release from the original tumor site as well as penetration and invasion of the vasculature. Because the long-term malignancy of sarcomas or other cancerous cells is related to their ability to metastasize, investigation of single-cell mechanics may provide new insights into the process of cell attachment, migration, and invasion from both a mechanistic as well as a diagnostic/prognostic standpoint (7,15).

The cell lines examined in this study have been well-characterized with respect to their chondrocytic differentiation, invasiveness, gene expression, and malignancy, with JJ012 cells showing the least chondrocytic differentiation, fastest doubling times, and highest malignancy, followed by FS090, and then 105KC in these characteristics (17–24). JJ012 were derived from a grade II, myxoid chondrosarcoma that exhibited aggressive metastasis. FS090 cells were established from a grade II, myxoid chondrosarcoma also exhibiting metastasis, but less aggressive than JJ012 cells. 105KC cells were also from a grade II, myxoid chondrosarcoma similar to the JJ012 line, but one which did not metastasize (17). Previous work has shown an inverse relationship between the malignancy of these cell lines and their degree of chondrocytic differentiation, and suggested that their metastatic ability was dependent on the expression of specific matrix metalloproteases such as collagenase (22,24) required for both egress from the primary tumor as well as invasion into the extracellular matrix remotely.

The mechanisms responsible for the differences in cell properties and metastatic potential among these cell lines remain to be determined. The findings of this study, taken together with previous studies, suggest that more aggressive,

TABLE 1 Time constants were measured for the AFM stress relaxation test, and Kelvin spring elements were calculated based on a standard linear solid model

	2 h			2 days		
	JJ012	FS090	105KC	JJ012	FS090	105KC
τ_σ (s)	16 ± 11	12 ± 8.0	16 ± 8.3	7.2 ± 5.2	7.9 ± 6.2	6.6 ± 5.3
τ_ε (s)	8.0 ± 5.1	6.6 ± 4.0	7.7 ± 4.2	5.2 ± 3.5	5.6 ± 4.3	4.4 ± 3.1
k_1 (Pa)	230 ± 150	850 ± 570	530 ± 220	770 ± 470	1230 ± 680	930 ± 670
k_2 (Pa)	210 ± 130	720 ± 710	530 ± 360	240 ± 170	390 ± 150	320 ± 180
$k_1 + k_2$ (Pa)	440 ± 270	1600 ± 1100	1100 ± 500	1000 ± 600	1600 ± 800	1200 ± 800
Elastic R^2	0.988 ± 0.014	0.981 ± 0.021	0.983 ± 0.021	0.996 ± 0.005	0.980 ± 0.022	0.989 ± 0.014
Viscoelastic R^2	0.889 ± 0.051	0.908 ± 0.037	0.902 ± 0.042	0.846 ± 0.101	0.748 ± 0.237	0.818 ± 0.143

R^2 values are given for both elastic and viscoelastic model fits.

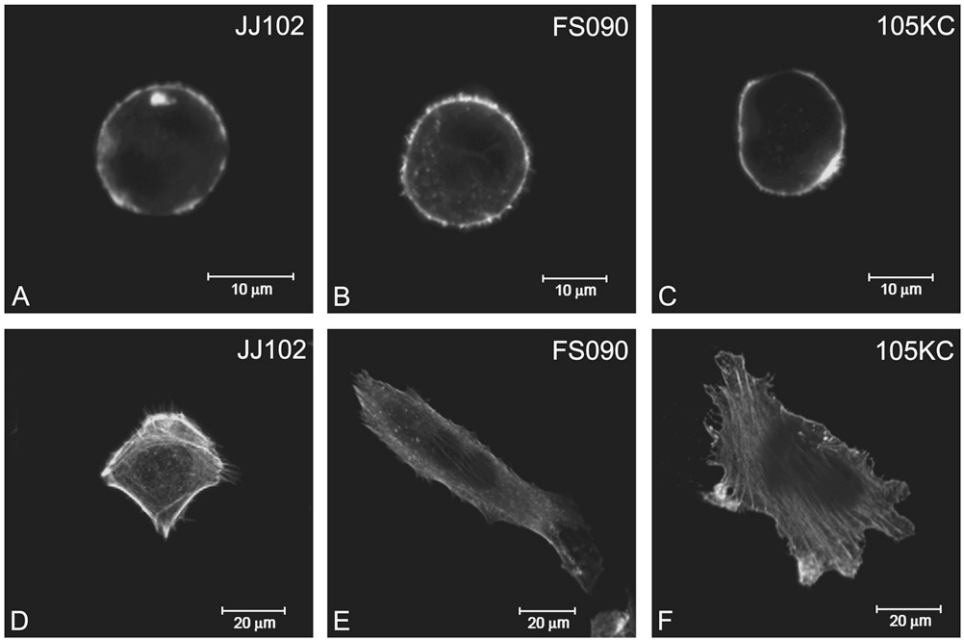

FIGURE 4 F-actin labeling of chondrosarcoma cells. Fluorescent labeling of cytoskeletal actin illustrated the typical cell morphologies seen at 2 h and 2 days. Cells retained a rounded shape ~13–16 μm in height at the early time point (*A*, *B*, and *C*) but spread out to ~6 μm in height by the late time point (*D*, *E*, and *F*).

metastatic chondrosarcoma lines are characterized by faster doubling times, higher migration rates (i.e., invasive ability), and lower elastic and viscoelastic moduli. Interestingly, reorganization of the cytoskeleton, and in particular the actin microfilaments, has been shown to play a critical role in all of these various characteristics (7,15,33–37). For example, hypoosmotic stress has been shown to cause a decrease in chondrocyte stiffness due to reorganization of the cortical F-actin structure (38–40). For this reason, we examined the organization of F-actin qualitatively in these cell lines to compare their cytoskeletal architecture. At 2 h, a cortical shell of F-actin existed for all cell lines, an observation that has also been made for other chondrocytic cells (33,38,40,41). This cytoskeletal arrangement altered significantly over 2 days as the cells spread and flattened on the culture surface. JJ012 and 105KC cells had similar structures, whereas FS090 cells tended to be elongated with large F-actin fibers extending longitudinally. These differences were reflected directly in the elastic and viscoelastic properties of the cells, which at 2 days were similar for JJ012 and 105KC, whereas the moduli of FS090 cells were greater. Similarly, FS090 cells showed significantly greater membrane area than the other cell lines. An alternative hypothesis for the larger moduli of flattened cells is a greater contribution to the mechanical properties by the nucleus, since the testing procedure was standardized by indenting cells only over the nucleus. Previous studies have shown that the chondrocyte nucleus is three to four times stiffer than the intact cell (42). Although the nucleus would play only a minor role in the observed mechanical properties of spherical cells, the thin flattened cells would see a larger contribution from the nucleus because it is partially indented during testing.

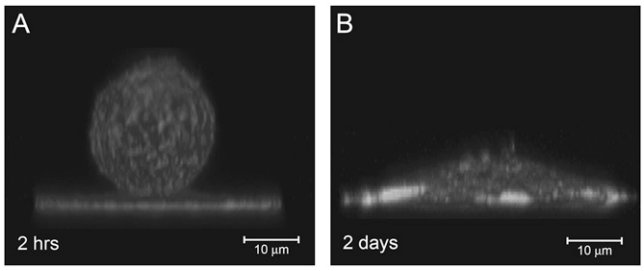

FIGURE 5 Chondrosarcoma morphology at 2 h and 2 days after seeding. Cells maintained a spherical shape when seeded onto PLL-coated, glass slides (*A*). Cytoskeletal F-actin was found peripherally, as well as in a thin layer where the cell attached to the surface. This layer continued to spread and thicken over time as the cell spread in culture (*B*).

An important advance of this study was the application of a thin-layer, AFM stress relaxation model for determining the viscoelastic properties of flattened, adherent cells. Although the sample height is not a concern for thick specimens such as tissues (43), significant errors may occur in these measurements for cells with heights of only a few microns. An important concern when conducting mechanical tests is to be conscious of the applied model's limitations. In this study, two time points were used to investigate the biomechanical properties of single, chondrosarcoma cells. The 2-h time point was chosen to investigate the mechanics of chondrosarcoma cells with a spherical morphology and is expected to yield measurements relatively independent of the substrate. Recent studies have shown that the substrate material can significantly influence the elastic properties of adherent cells (44). It is important, however, to note that the goal of this study was to compare the properties of the different cell lines, as opposed to the different culture conditions and respective cell morphologies. Because of the large cell heights that existed initially, strains for the 2-h tests were well within the model's range of

validity. The 2-day time point was chosen to allow the cells to spread and obtain morphologies more typical of chondrosarcomas in vivo. Strains in these tests were occasionally higher (~10–15%) and could pose a possible source of error for the reported values at 2 days. The model used in this study assumed small strains during indentation, and although most tests produced strains below 10%, some exceeded this limit, which could cause second order errors to be introduced into the final values. However, these errors were on the order of a few percent and would be expected to be similar among the sample groups. Importantly, the development of a new mathematical model suitable for thin-layer, AFM stress relaxation tests will not only allow testing of spread adherent cells, but also could be used to investigate other anchorage-dependent cell types in addition to thin biomaterials and polymeric coatings.

The biomechanical properties extracted from the elastic and viscoelastic analyses showed slight differences that could be attributed to limitations in the experimental setup. As data for the elastic and viscoelastic tests were collected using two different sampling rates (2 kHz and 100 Hz, respectively) in two subsequent tests, the probe-cell contact point may have differed slightly for the two analyses of a common cell. This discrepancy introduced error that accounts for the aberrations seen in the results, specifically that $E_{elastic}$ and E_Y are not identical and that E_{equil} is larger than $E_{elastic}$ at 2 days. Neither of these differences were statistically significant, however, and because the error was consistent for all cell lines and morphologies, the relative differences between cell lines should still be valid. Future experiments will account for this source of experimental error by collecting elastic and viscoelastic data from a single indentation test at a higher sampling rate.

Although there are no previous reports on the biomechanical properties of chondrosarcoma cells, single-cell studies have been conducted on a variety of other chondrocytic cells, showing properties that are consistent with this study. Porcine articular chondrocytes tested using this AFM technique showed properties on the same order of magnitude, with equilibrium moduli of 0.17–0.31 kPa, instantaneous moduli of 0.29–0.55 kPa, and apparent viscosities of 0.61–1.15 kPa·s (27). Similar elastic properties (~0.5 kPa) were measured for bovine chondrocytes using AFM with pyramidal tips (39). Micropipette aspiration testing of human chondrocytes produced similar results, with equilibrium moduli of 0.24 kPa, instantaneous moduli of 0.41 kPa, and apparent viscosities of 3.0 kPa·s (30). Studies investigating other musculoskeletal cell types found a range of mechanical properties that were typically higher than those of chondrocytes. AFM indentation on the nuclear region of osteoblasts produced an elastic modulus ranging from 1 to 14 kPa (4,44), whereas fibroblasts had an elastic modulus of 4 kPa when tested at the same location (45). The cellular mechanics of smooth muscle cells have also been investigated using AFM, with elastic moduli being reported in the range of 12–45 kPa (46). The large discrepancies in these different measurements may reflect both intrinsic differences among cell types, as well as biomechanical testing at different scales depending on the size of the AFM tip. The properties measured in this study correspond most closely with articular chondrocytes and fibroblasts, indicating that chondrosarcoma cells may share some mechanical traits with these cells.

In previous studies on other cell lines, a direct correlation was found between increasing deformability and the progression of a fibroblast cell line from a normal to a tumorigenic phenotype (47). Transformed fibroblasts were also shown to have lower apparent viscosities than normal cells and exhibit less contractility when tested in suspension (48). Furthermore, micropipette aspiration experiments showed that transformed fibroblasts exhibiting the metastatic phenotype detached from surfaces more easily and were ~50% more deformable than normal cells (49). These conclusions are consistent with the findings of this study, which suggest that cell transformation and tumorigenicity are associated with a decrease in cell modulus and apparent viscosity.

The results of this study indicate that significant differences may exist in cellular mechanical properties among different chondrosarcoma cell lines of varying malignancy. These findings, along with previous biochemical results, may provide new diagnostic or prognostic approaches for determining the metastatic potential of chondrosarcoma or other cancerous cells. For example, recent studies have reported the use of an optical trap to rapidly sort a population of cells based on their deformability (7). Furthermore, an improved understanding of the mechanisms responsible for these alterations in mechanical properties with transformation may provide new insight into the development of pharmacologic approaches for inhibiting metastasis by chemically targeting cytoskeletal structures that regulate cell stiffness and motility, such as F-actin (15,34–36).

We thank Matthew Topel for assistance with analyzing the stress relaxation data, and Dr. H. Ping Ting-Beall for performing the membrane area experiments.

This work was supported in part by National Institutes of Health grants EB01630, AG15768, AR48182, and AR50245.

REFERENCES

1. Hochmuth, R. M. 2000. Micropipette aspiration of living cells. *J. Biomech.* 33:15–22.
2. Evans, E., and A. Yeung. 1989. Apparent viscosity and cortical tension of blood granulocytes determined by micropipet aspiration. *Biophys. J.* 56:151–160.
3. Mahaffy, R. E., S. Park, E. Gerde, J. Kas, and C. K. Shih. 2004. Quantitative analysis of the viscoelastic properties of thin regions of fibroblasts using atomic force microscopy. *Biophys. J.* 86:1777–1793.
4. Charras, G. T., and M. A. Horton. 2002. Determination of cellular strains by combined atomic force microscopy and finite element modeling. *Biophys. J.* 83:858–879.
5. Shin, D., and K. Athanasiou. 1999. Cytoindentation for obtaining cell biomechanical properties. *J. Orthop. Res.* 17:880–890.
6. Bausch, A. R., F. Ziemann, A. A. Boulbitch, K. Jacobson, and E. Sackmann. 1998. Local measurements of viscoelastic parameters of adherent cell surfaces by magnetic bead microrheometry. *Biophys. J.* 75:2038–2049.
7. Guck, J., S. Schinkinger, B. Lincoln, F. Wottawah, S. Ebert, M. Romeyke, D. Lenz, H. M. Erickson, R. Ananthakrishnan, D. Mitchell,

and others. 2005. Optical deformability as an inherent cell marker for testing malignant transformation and metastatic competence. *Biophys. J.* 88:3689–3698.

8. Costa, K. D., and F. C. Yin. 1999. Analysis of indentation: implications for measuring mechanical properties with atomic force microscopy. *J. Biomech. Eng.* 121:461–471.
9. Domke, J., and M. Radmacher. 1998. Measuring the elastic properties of thin polymer films with the atomic force microscope. *Langmuir.* 14: 3320–3325.
10. Costa, K. D. 2003. Single-cell elastography: probing for disease with the atomic force microscope. *Dis. Markers.* 19:139–154.
11. Guilak, F. 2000. The deformation behavior and viscoelastic properties of chondrocytes in articular cartilage. *Biorheology.* 37:27–44.
12. Huang, H., R. D. Kamm, and R. T. Lee. 2004. Cell mechanics and mechanotransduction: pathways, probes, and physiology. *Am. J. Physiol. Cell Physiol.* 287:C1–11.
13. Ingber, D. E. 2003. Mechanobiology and diseases of mechanotransduction. *Ann. Med.* 35:564–577.
14. Zhu, C., G. Bao, and N. Wang. 2000. Cell mechanics: mechanical response, cell adhesion, and molecular deformation. *Annu. Rev. Biomed. Eng.* 2:189–226.
15. Yamazaki, D., S. Kurisu, and T. Takenawa. 2005. Regulation of cancer cell motility through actin reorganization. *Cancer Sci.* 96:379–386.
16. Weber, K. L. 2005. What's new in musculoskeletal oncology. *J. Bone Joint Surg. Am.* 87:1400–1410.
17. Martin, J. A., E. Forest, J. A. Block, A. J. Klingelhutz, B. Whited, S. Gitelis, A. Wilkey, and J. A. Buckwalter. 2002. Malignant transformation in human chondrosarcoma cells supported by telomerase activation and tumor suppressor inactivation. *Cell Growth Differ.* 13:397–407.
18. Block, J. A., S. E. Inerot, and J. H. Kimura. 1992. Heterogeneity of keratan sulfate substituted on human chondrocytic large proteoglycans. *J. Biol. Chem.* 267:7245–7252.
19. Ghert, M. A., W. N. Qi, H. P. Erickson, J. A. Block, and S. P. Scully. 2001. Tenascin-C splice variant adhesive/anti-adhesive effects on chondrosarcoma cell attachment to fibronectin. *Cell Struct. Funct.* 26:179–187.
20. Jagasia, A. A., J. A. Block, M. O. Diaz, T. Nobori, S. Gitelis, S. E. Inerot, and A. P. Iyer. 1996. Partial deletions of the CDKN2 and MTS2 putative tumor suppressor genes in a myxoid chondrosarcoma. *Cancer Lett.* 105:77–90.
21. Jagasia, A. A., J. A. Block, A. Qureshi, M. O. Diaz, T. Nobori, S. Gitelis, and A. P. Iyer. 1996. Chromosome 9 related aberrations and deletions of the CDKN2 and MTS2 putative tumor suppressor genes in human chondrosarcomas. *Cancer Lett.* 105:91–103.
22. Jiang, X., C. M. Dutton, W. N. Qi, J. A. Block, N. Garamszegi, and S. P. Scully. 2005. siRNA mediated inhibition of MMP-1 reduces invasive potential of a human chondrosarcoma cell line. *J. Cell. Physiol.* 202:723–730.
23. Schorle, C. M., F. Finger, A. Zien, J. A. Block, P. M. Gebhard, and T. Aigner. 2005. Phenotypic characterization of chondrosarcoma-derived cell lines. *Cancer Lett.* 226:143–154.
24. Scully, S. P., K. R. Berend, A. Toth, W. N. Qi, Z. Qi, and J. A. Block. 2000. Marshall Urist Award. Interstitial collagenase gene expression correlates with in vitro invasion in human chondrosarcoma. *Clin. Orthop.* 376:291–303.
25. Wyckoff, J. B., J. G. Jones, J. S. Condeelis, and J. E. Segall. 2000. A critical step in metastasis: in vivo analysis of intravasation at the primary tumor. *Cancer Res.* 60:2504–2511.
26. Shah-Yukich, A. A., and A. C. Nelson. 1988. Characterization of solid tumor microvasculature: a three-dimensional analysis using the polymer casting technique. *Lab. Invest.* 58:236–244.
27. Darling, E. M., S. Zauscher, and F. Guilak. 2006. Viscoelastic properties of zonal articular chondrocytes measured by atomic force microscopy. *Osteoarthritis Cartilage.* 14:571–579.
28. Hutter, J. L., and J. Bechhoefer. 1993. Calibration of atomic-force microscope tips. *Rev. Sci. Instrum.* 64:1868–1873.
29. Jones, W. R., H. P. Ting-Beall, G. M. Lee, S. S. Kelley, R. M. Hochmuth, and F. Guilak. 1999. Alterations in the Young's modulus and volumetric properties of chondrocytes isolated from normal and osteoarthritic human cartilage. *J. Biomech.* 32:119–127.
30. Trickey, W. R., G. M. Lee, and F. Guilak. 2000. Viscoelastic properties of chondrocytes from normal and osteoarthritic human cartilage. *J. Orthop. Res.* 18:891–898.
31. Dimitriadis, E. K., F. Horkay, J. Maresca, B. Kachar, and R. S. Chadwick. 2002. Determination of elastic moduli of thin layers of soft material using the atomic force microscope. *Biophys. J.* 82:2798–2810.
32. Johnson, K. L. 1985. Contact Mechanics. Cambridge University Press, Cambridge, United Kingdom.
33. Guilak, F., G. R. Erickson, and H. P. Ting-Beall. 2002. The effects of osmotic stress on the viscoelastic and physical properties of articular chondrocytes. *Biophys. J.* 82:720–727.
34. Donald, C. D., C. R. Cooper, S. Harris-Hooker, N. Emmett, M. Scanlon, and D. B. Cooke III. 2001. Cytoskeletal organization and cell motility correlates with metastatic potential and state of differentiation in prostate cancer. *Cell Mol. Biol.* (Noisy-le-grand) 47:1033–8.
35. Korb, T., K. Schluter, A. Enns, H. U. Spiegel, N. Senninger, G. L. Nicolson, and J. Haier. 2004. Integrity of actin fibers and microtubules influences metastatic tumor cell adhesion. *Exp. Cell Res.* 299:236–247.
36. Lambrechts, A., M. Van Troys, and C. Ampe. 2004. The actin cytoskeleton in normal and pathological cell motility. *Int. J. Biochem. Cell Biol.* 36:1890–1909.
37. Trickey, W. R., T. P. Vail, and F. Guilak. 2004. The role of the cytoskeleton in the viscoelastic properties of human articular chondrocytes. *J. Orthop. Res.* 22:131–139.
38. Erickson, G. R., D. L. Northrup, and F. Guilak. 2003. Hypo-osmotic stress induces calcium-dependent actin reorganization in articular chondrocytes. *Osteoarthritis Cartilage.* 11:187–197.
39. Hung, C. T., K. D. Costa, and X. E. Guo. 2001. Apparent and transient mechanical properties of chondrocyte during osmotic loading using triphasic theory and AFM indentation. *ASME Bioengineering Conference*, 50:625–6.
40. Pritchard, S., and F. Guilak. 2004. The role of F-actin in hypo-osmotically induced cell volume change and calcium signaling in anulus fibrosus cells. *Ann. Biomed. Eng.* 32:103–111.
41. Erickson, G. R., L. G. Alexopoulos, and F. Guilak. 2001. Hyper-osmotic stress induces volume change and calcium transients in chondrocytes by transmembrane, phospholipid, and G-protein pathways. *J. Biomech.* 34:1527–1535.
42. Guilak, F., J. R. Tedrow, and R. Burgkart. 2000. Viscoelastic properties of the cell nucleus. *Biochem. Biophys. Res. Commun.* 269:781–786.
43. Allen, D. M., and J. J. Mao. 2004. Heterogeneous nanostructural and nanoelastic properties of pericellular and interterritorial matrices of chondrocytes by atomic force microscopy. *J. Struct. Biol.* 145:196–204.
44. Takai, E., K. D. Costa, A. Shaheen, C. T. Hung, and X. E. Guo. 2005. Osteoblast elastic modulus measured by atomic force microscopy is substrate dependent. *Ann. Biomed. Eng.* 33:963–971.
45. Haga, H., S. Sasaki, K. Kawabata, E. Ito, T. Ushiki, and T. Sambongi. 2000. Elasticity mapping of living fibroblasts by AFM and immunofluorescence observation of the cytoskeleton. *Ultramicroscopy.* 82: 253–258.
46. Collinsworth, A. M., S. Zhang, W. E. Kraus, and G. A. Truskey. 2002. Apparent elastic modulus and hysteresis of skeletal muscle cells throughout differentiation. *Am. J. Physiol. Cell Physiol.* 283:C1219–C1227.
47. Ward, K. A., W. I. Li, S. Zimmer, and T. Davis. 1991. Viscoelastic properties of transformed cells: role in tumor cell progression and metastasis formation. *Biorheology.* 28:301–313.
48. Thoumine, O., and A. Ott. 1997. Comparison of the mechanical properties of normal and transformed fibroblasts. *Biorheology.* 34:309–326.
49. Anderson, K. W., W. I. Li, J. Cezeaux, and S. Zimmer. 1991. In vitro studies of deformation and adhesion properties of transformed cells. *Cell Biophys.* 18:81–97.